

VIP Very Important Paper

Structural and Mutagenesis Studies of the Thiamine-Dependent, Ketone-Accepting YerE from *Pseudomonas protegens*

Sabrina Hampel^{+, [a]} Jan-Patrick Steitz^{+, [a]} Anna Baierl^{+, [b]} Patrizia Lehwald,^[a] Luzia Wiesli,^[c] Michael Richter,^[c, d] Alexander Fries,^[a] Martina Pohl,^[b] Gunter Schneider,^[e] Doreen Dobritzsch,^{*[f]} and Michael Müller^{*[a]}

A wide range of thiamine diphosphate (ThDP)-dependent enzymes catalyze the benzoin-type carbonylation of pyruvate with aldehydes. A few ThDP-dependent enzymes, such as YerE from *Yersinia pseudotuberculosis* (YpYerE), are known to accept ketones as acceptor substrates. Catalysis by YpYerE gives access to chiral tertiary alcohols, a group of products difficult to obtain in an enantioenriched form by other means. Hence, knowledge of the three-dimensional structure of the enzyme is crucial to identify structure–activity relationships. However,

YpYerE has yet to be crystallized, despite several attempts. Herein, we show that a homologue of YpYerE, namely, PpYerE from *Pseudomonas protegens* (59% amino acid identity), displays similar catalytic activity: benzaldehyde and its derivatives as well as ketones are converted into chiral 2-hydroxy ketones by using pyruvate as a donor. To enable comparison of aldehyde- and ketone-accepting enzymes and to guide site-directed mutagenesis studies, PpYerE was crystallized and its structure was determined to a resolution of 1.55 Å.

Introduction

YerE from *Yersinia pseudotuberculosis* (YpYerE) was the first characterized biocatalyst for thiamine diphosphate (ThDP)-dependent aldehyde–ketone cross-coupling.^[1,2] YpYerE is involved in the biosynthesis of the branched-chain sugar yersiniose A, which is part of the O-antigen of the host and other bacteria.^[1,3] The physiologically catalyzed reaction is the transfer of an activated acetaldehyde, generated by decarboxylation of

pyruvate, to a 3,6-dideoxy-4-keto sugar.^[1] In addition to pyruvate, YpYerE accepts 2-oxobutyrate and acetaldehyde as donors and a broad range of different acceptor substrates with moderate to high enantioselectivity.^[2]

In addition to YpYerE, other ThDP-dependent enzymes are able to accept ketones. Acetohydroxy acid synthases (AHASs) are a large group of ThDP-dependent enzymes that are distantly related to YerE. Physiologically, they catalyze the synthesis of acetolactate and acetohydroxy acids.^[4,5] AHASs accept α -keto acids but are not known to accept nonactivated ketones.

The enzyme acetoin:dichlorophenolindophenol oxidoreductase (Ao:DCPIP OR) from *Bacillus licheniformis* [also named acetylacetoin synthase (AAS)^[4,6,7]] is able to activate and transfer 2-hydroxy ketones, for example, acetoin and methylacetoin, as well as 1,2-diketones of different chain lengths (C₂ and C₃). Moreover, as with YpYerE, esters of pyruvate can act as acceptor substrates. Compared to YpYerE, Ao:DCPIP OR affords the same enantioselectivity for the addition of acetaldehyde to cyclohexane-1,2-dione but opposite enantiomers with aromatic acceptor substrates.^[5] Recently, Giovannini et al. reported the highly enantioselective synthesis of (S)-phenylacetylcarbinol [(S)-PAC] and its derivatives in good yields by the wild-type Ao:DCPIP OR using methylacetoin as a donor substrate.^[8] Before that, the synthesis of (S)-PAC was achieved only by rationally designed variants of R-selective enzymes.^[9]

The related enzyme AcoAB from *Bacillus subtilis* plays a key role in the biodegradation of methylacetoin. Metabolic engineering proved its ability to generate an activated acetaldehyde from pyruvate or acetoin that is transferred to acetone, generating methylacetoin.^[10] The range of donor and acceptor

[a] Dr. S. Hampel,⁺ J.-P. Steitz,⁺ Dr. P. Lehwald, Dr. A. Fries, Prof. Dr. M. Müller
Institut für Pharmazeutische Wissenschaften, Albert-Ludwigs-Universität
Freiburg, Albertstrasse 25, 79104 Freiburg (Germany)
E-mail: michael.mueller@pharmazie.uni-freiburg.de

[b] A. Baierl,⁺ Prof. Dr. M. Pohl
IBG-1: Biotechnology, Forschungszentrum Jülich GmbH
Wilhelm-Johnen Str., 52425 Jülich (Germany)

[c] L. Wiesli, Dr. M. Richter
Empa - Swiss Federal Laboratories for Materials Science and Technology
Laboratory for Biointerfaces
Lerchenfeldstrasse 5, 9014 St. Gallen (Switzerland)

[d] Dr. M. Richter
Fraunhofer Institute for Interfacial Engineering and Biotechnology IGB,
Branch BioCat, Schulgasse 11a, 94315 Straubing (Germany)

[e] Prof. Dr. G. Schneider
Department of Medical Biochemistry and Biophysics, Karolinska Institutet
Tomtebodavägen 6, 17177 Stockholm (Sweden)

[f] Assoc. Prof. D. Dobritzsch
Visiting address: Department of Chemistry-BMC, Uppsala Universitet
Husargatan 3, 75237 Uppsala (Sweden)
E-mail: doreen.dobritzsch@kemi.uu.se

[*] These authors contributed equally to this work.

Supporting Information and the ORCID identification numbers for the authors of this article can be found under
<https://doi.org/10.1002/cbic.201800325>.

substrates and reactivities is rarely comparable with those of YpYerE.

ThDP-dependent cyclohexane-1,2-dione hydrolase (CDH) from *Azoarcus* sp. strain 22Lin, similar to lolD from different organisms, might play a role in the catabolism of cyclitols and inositols. CDH catalyzes the cleavage of C–C bonds and can catalyze the reverse reaction. The double variant CDH-H28A/N484A was rationally created to accept ketones as acceptor substrates; this variant shares an overlapping substrate range with YpYerE. Two notable donor substrates accepted by the double variant are methyl pyruvate and butane-2,3-dione. This reactivity is similar to that of the enzymes from acetoin metabolism.^[11,12]

Despite its fundamental biocatalytic and biosynthetic significance, YpYerE has not been structurally characterized as of yet, although numerous attempts to obtain crystals have been made. Within this paper, we present our efforts to gain deeper insight into the catalysis of ketone-accepting, ThDP-dependent enzymes by identifying an enzyme homologous to YpYerE, PpYerE from *Pseudomonas protegens*, for which we were able to obtain crystals suitable for X-ray structure elucidation; this enzyme shows homology to YpYerE in terms of the associated biosynthetic gene cluster and the reactions catalyzed.

Results and Discussion

We identified the putative enzyme PpYerE by BLAST analysis using the protein sequence of YpYerE. Both proteins are nearly equal in length with 568 and 565 amino acids, respectively, of which 336 are identical (59.3%).^[13] The biosynthetic gene clusters for the synthesis of yersiniose A and ascarylose were ana-

lyzed and compared with the putative biosynthetic gene cluster containing the *pp-yerE* gene on the genetic level.^[1,14] Ascarylose is a 3,6-dideoxysugar included in the O-antigen of different *Y. pseudotuberculosis* strains.

Chen et al. identified four homologous genes in the biosynthetic gene clusters of yersiniose A and ascarylose.^[1] Those genes (*ddhA-D*) encode four enzymes that catalyze the conversion of α -D-glucose 1-phosphate (1) into CDP-4-keto-3,6-dideoxy-D-glucose (2), namely, α -D-glucose-1-phosphate cytidyltransferase (E_p), CDP-D-glucose-4,6-dehydratase (E_{od}), CDP-6-deoxy-L-threo-D-glycero-4-hexulose-3-dehydratase (E_1), and CDP-6-deoxy-L-threo-D-glycero-4-hexulose-3-dehydratase reductase (E_3) (Figure 1 A).^[15] Four similar genes are also part of a homologous biosynthetic gene cluster of *P. protegens* and, moreover, are arranged in the same order. Comparison of each translated protein gives amino-acid sequence identities of 40–80% compared to the proteins from the yersiniose A biosynthetic gene cluster (Figure 1 B). From this observation, we conclude that the substrate biosynthetically converted by PpYerE is likely CDP-4-keto-3,6-dideoxy-D-glucose (2) or a related keto sugar.

In the biosynthesis of CDP-yersiniose A (4), the coupling of CDP-4-keto-3,6-dideoxy-D-glucose (2) and the ThDP-bound activated acetaldehyde is followed by reduction of ketone 3.^[1] Chen et al. postulated that YpYerF, an NAD(P)H-dependent reductase, catalyzes this reaction.^[1] A gene (*pp-yerF*) with moderate identity to *yp-yerF* (37%) was found. The gene product, annotated as an epimerase, was named PpYerF. Further in silico investigation has not given conclusive proof of its function. Nevertheless, the low sequence homology to *ascE* (25%), the epimerase from the ascarylose biosynthetic gene cluster, is

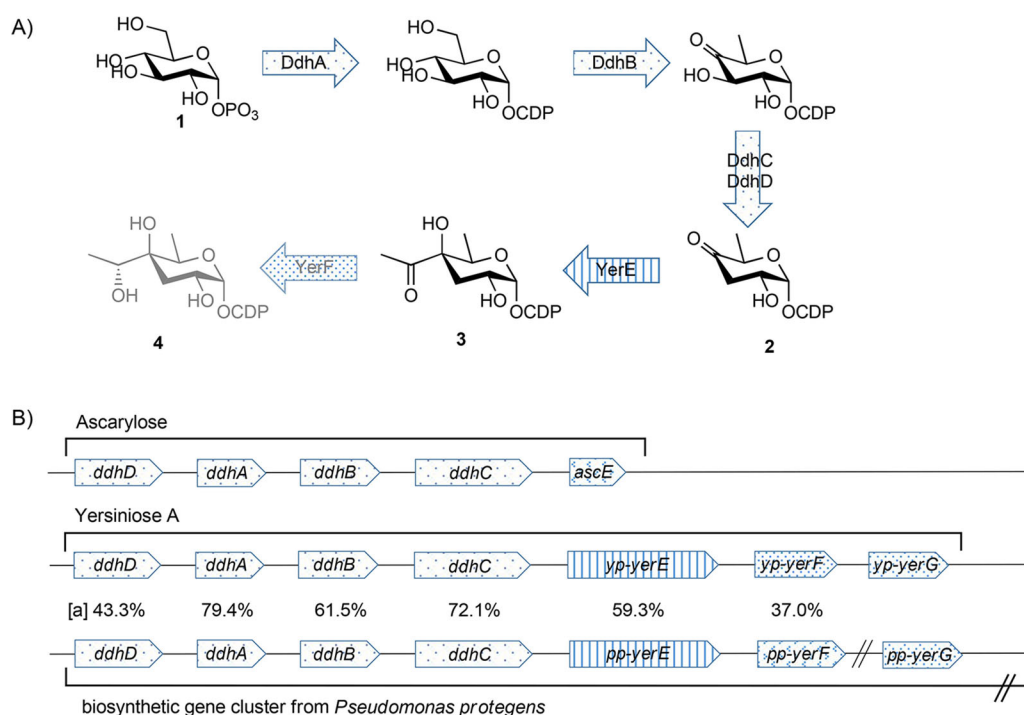


Figure 1. A) Biosynthesis of cytidine diphosphate (CDP)-yersiniose A (4) according to Chen et al. B) Schematic representation of the biosynthetic gene cluster of ascarylose and yersiniose A compared to a section of the cluster harboring PpYerE. [a] Percentage of identity between translated genes of *Y. pseudotuberculosis* O:VI and *P. protegens*.

noteworthy.^[1,13,14] We found four open reading frames in the biosynthetic gene cluster harboring the *pp-yerE* gene that possibly code for glycosyltransferases; however, none of them showed any homology to YerG. Another open reading frame encodes conserved domains that are common in acyltransferases.

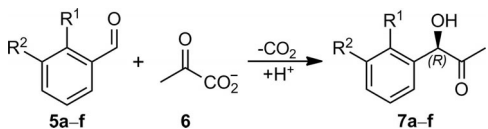
Regrettably, the structure of the physiological donor substrate could not be directly deduced from sequence analysis of the biosynthetic gene cluster. We did not find any genes encoding enzymes that might play a role in the synthesis of a donor substrate other than pyruvate, for example, an aldolase that chain elongates pyruvate. As pyruvate was a good donor in the *in vitro* assays (see below) and is ubiquitous in the cell, we propose that pyruvate is the physiological donor substrate of *PpYerE*.

To gain deeper insight into the catalytic mechanism of ketone-accepting ThDP-dependent enzymes, we investigated whether *PpYerE* could substitute *YpYerE* in several of the reactions known to be catalyzed by the latter, with pyruvate or acetaldehyde being used as the donor substrate.

Formation of phenylacetylcarbinol (PAC, 7)

The synthesis of PAC and derivatives thereof from benzaldehydes **5** and pyruvate (**6**) can be performed by using well-known reactions catalyzed by many ThDP-dependent enzymes.^[16] Benzaldehydes **5a–f** were accepted and nearly quantitatively converted into the *R* enantiomer of PAC and respective derivatives **7a–f** by *PpYerE* as well as *YpYerE* (Table 1). For the studied conversions, the enantioselectivity of *PpYerE* was significantly lower, except for the reaction of 3-hydroxybenzaldehyde (**5f**) with **6** (Table 1). However, we observed a steady decrease in the enantiomeric excess (*ee*) in the products over time. We also observed a decrease of the *ee* of previously purified (*R*)-PAC (**7a**; without enzyme) after 1, 3, and 24 h in buffer from > 99 to 98, and 94% *ee*, respectively.

Table 1. Enzymatic synthesis of PAC and derivatives **7a–f** by *PpYerE* and *YpYerE*.^[a]



	a	b	c	d	e	f
R ¹ , R ²	H, H	F, H,	Cl, H	Br, H	I, H	H, OH
<i>PpYerE</i>						
<i>ee</i> [%] (24 h)	84	76	74	74	68	75
conversion [%] (48 h)	96	97	98	99	>99	>99
<i>YpYerE</i>						
<i>ee</i> [%] (24 h)	97	94	94	94	80	61
conversion [%] (48 h)	82	98	97	97	95	88

[a] Conditions: benzaldehyde or derivative **5a–f** (20 mM), pyruvate (**6**, 50 mM), *PpYerE* [1.0 mg mL⁻¹ (Bradford)], *YpYerE* (crude extract), 20–30% DMSO, KP, buffer (50 mM, pH 8.0, containing 3 mM MgCl₂, 0.5 mM ThDP), 30 °C. Conversion was determined by GC–MS analysis; *ee* was determined by chiral-phase HPLC.

Formation of acetolactate and acetoin

Incubation of *PpYerE* with pyruvate (**6**) as the sole substrate yielded nearly racemic acetoin. Experiments with [2-¹³C]-**6** showed the enzymatic synthesis of acetolactate, followed by a probably non-enzymatic decarboxylation. This is in line with the (low) enantioselectivity observed for the enzymatic reaction of two molecules of acetaldehyde [(*S*)-acetoin, 26% *ee*] and of pyruvate (**6**) and acetaldehyde [(*S*)-acetoin, 21% *ee*].

For *YpYerE*, the formation of both products of the homocoupling of pyruvate (**6**), acetolactate, and acetoin was also shown. The ¹H NMR spectroscopy data (in D₂O) indicated the quantitative synthesis of acetolactate, and we also identified small amounts of acetoin. After extraction with ethyl acetate, only the decarboxylation product acetoin (< 5% *ee*) was identified, which was probably due to the low solubility of acetolactate in ethyl acetate. Hence, the mechanism for acetolactate formation followed by non-enzymatic decarboxylation to yield nearly racemic acetoin is assumed to be the same for both enzymes.

Cross-coupling of aldehydes and (di)ketones

For the synthesis of tertiary alcohols, different cyclic and acyclic ketones were studied, and most of them were known substrates of *YpYerE* (for all tested ketones, see Table S3 in the Supporting Information). Pyruvate (**6**) was used as a donor substrate.

The selectivities for cyclic ketones differed between *PpYerE* and *YpYerE*: the conversion of cyclohexanone (**8**) was lower with *PpYerE* than with *YpYerE*, whereas cyclopentanone and cycloheptanone were not accepted at all. Both *YpYerE* and *PpYerE* did not accept cyclooctanone or α -tetralone [3,4-dihydro-1(2*H*)-naphthalenone]. Cyclohexane-1,2-dione (**9**) was a substrate of *PpYerE*, but a low conversion (5%) was observed even after variation of the substrate ratios. β -Tetralone [3,4-dihydro-2(1*H*)-naphthalenone, **10**] was converted by *PpYerE* to give 37% of tertiary alcohol **14** with 48% *ee*. In the analogous transformation by *YpYerE*, the conversion was higher (75%), yet the enantioselectivity was lower (9% *ee*). Hexane-3,4-dione (**18**) was converted by *PpYerE*, but the yield was lower (Table 2) than that given by *YpYerE*. In this case, both products showed the same absolute *S* stereochemistry with an inverse specific optical rotation relative to the product obtained by Ao:DCPIP OR catalysis.^[6] The conversion and enantioselectivity with 1-phenoxypropan-2-one (**11**) were lower with *PpYerE* catalysis than with *YpYerE* catalysis (Scheme 1, Table S3).

In summary, *YpYerE* and *PpYerE* exhibit high amino acid sequence identity, are located in homologous biosynthetic gene clusters, and, in general, behave similarly with respect to substrate range and stereoselectivity in biocatalytic C–C bond formation. Most probably, these enzymes are homologues and are involved in the biosynthesis of yersiniose or a structurally related derivative. Hence, we set out to elucidate the structures of both enzymes but obtained crystals only of *PpYerE*.

Table 2. Enantioselectivity of *PpYerE* variants for the carboligation of pyruvate (**6**) with benzaldehyde (**5a**), propanal (**16**), *n*-pentanal (**17**), and 3,4-hexanedione (**18**).^[a]

$$\text{R}^1\text{C}(=\text{O})\text{R}^2 + \text{CH}_3\text{C}(=\text{O})\text{CO}_2^- \xrightarrow[\text{+H}^+]{\text{CO}_2, \text{PpYerE}} \text{product}$$

Product	R ¹ , R ²	<i>PpYerE</i>		<i>PpYerE</i> V479A		<i>PpYerE</i> V479G	
		<i>ee</i> [%]	Conv. [%]	<i>ee</i> [%]	Conv. [%]	<i>ee</i> [%]	Conv. [%]
	Ph, H	> 99 (<i>R</i>)	99	95 (<i>R</i>)	88	> 99 (<i>R</i>)	97
	Et, H	40 (<i>S</i>)	n.d.	57 (<i>S</i>)	n.d.	55 (<i>R</i>)	n.d.
	<i>n</i> Bu, H	16 (<i>R</i>)	98	31 (<i>S</i>)	30	29 (<i>R</i>)	14
	EtCO, Et	19 ^[b]	n.d.	-27 ^[b]	n.d.	-4 ^[b]	n.d.

[a] Conditions: acceptor substrate (20–50 mM), pyruvate (**6**, 50 mM), *PpYerE* variant (1.0 mg mL⁻¹), 30 °C. Conversions were determined after 1 h by HPLC for aromatic products and by GC–MS for aliphatic products; *ee* values were determined after 1 h by chiral-phase HPLC or chiral-phase GC–MS analysis; n.d.: not determined. [b] For reactions with hexane-3,4-dione (**18**), the *ee* value was measured after 24 h.

Structure determination and quality of the models

Crystals of N-terminally His-tagged, full-length *PpYerE* (2 × 588 amino acids, 129.7 kDa) were grown in the presence of 3 mM MgCl₂ and 1 mM ThDP by using PEG-4000 as a precipitant. They diffract to 1.55 Å resolution, belong to space group *P2*₁, and contain two polypeptide chains (one homodimer) per asymmetric unit. With the unit-cell dimension *a* being equal in length to *c*, these crystals fulfill one of the possible sets of requirements that allow twinning in the *P2*₁ space group, and twinning was indeed observed. Structure determination was achieved by molecular replacement by using a subunit of *Arabidopsis thaliana* AHAS (PDB ID: 1YBH, 32% sequence identity) as a search model.

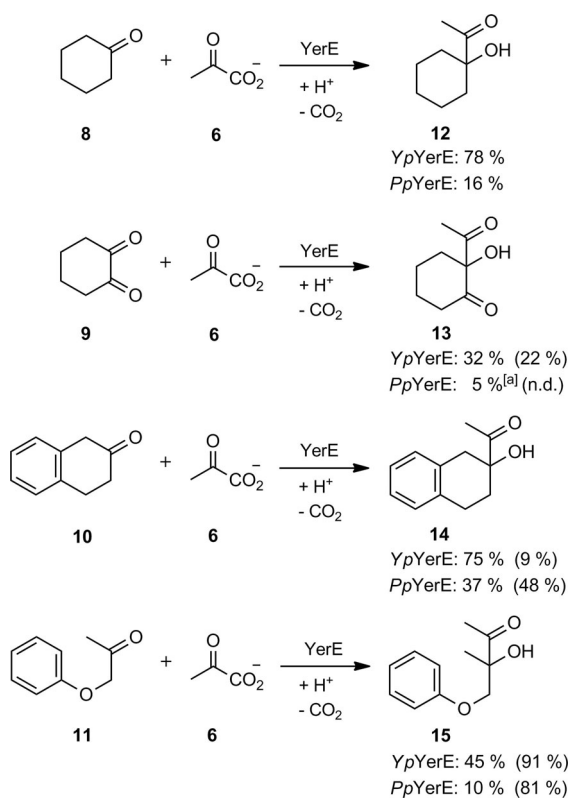
The final model was refined to $R_{\text{cryst}}/R_{\text{free}}$ values of 15.1%/17.4% and has excellent stereochemistry (Table S1). It contains one flavin adenine dinucleotide (FAD), one ThDP, and one magnesium ion per chain and a total of 878 water molecules. The observed electron density is well defined for all cofactors and almost the entire polypeptide chain, with the exception of an approximately ten-residue stretch that links the first two domains in both subunits (A183–192, B182–194) and parts of a loop and helix located at the entrance to the active site in chain B (B483–491). The N-terminal His tags, as well as the three C-terminal residues of chain A, are not visible in the electron-density map.

Overall structure

The structures of the two crystallographically independent monomers per asymmetric unit are essentially identical, with a root-mean-square deviation (RMSD) for the corresponding C_α positions of 0.22 Å. The fold of the *PpYerE* subunit closely resembles that of other ThDP-dependent enzymes. It is divided into three domains called Pyr or α domain (1–182), central or β domain (193–363), and PP or γ domain (364–568). All have an α/β-architecture comprising a central six-stranded, parallel β sheet with several helices packed against both sides (Figure 2).

PpYerE is a homodimer in the crystalline state and in solution (Figure 2A), a feature it shares with, for example, transketolase but not the majority of known ThDP-dependent enzymes, which instead are homotetramers assembled from two such dimers. The mode of dimer assembly is shared by all ThDP-dependent enzymes and is also conserved in *PpYerE*; the interface is formed between the respective Pyr and PP domains of the two monomers. It buries approximately 3400 Å² (15.8%) of the solvent-accessible surface area of each monomer and involves the formation of 57 hydrogen bonds and two salt bridges.

The closest structural homologue to *PpYerE* is, according to the criteria used by PDBeFOLD, the *Pseudomonas fluorescens* benzaldehyde lyase (BAL; PDB entry 2ag0, 25.3% sequence identity), which shows a Q-score of 0.60 and a RMSD of 1.8 Å for 501 aligned C_α atoms. BAL is a homotetrameric enzyme that does not bind FAD. Accordingly, the largest structural de-



Scheme 1. Ketone substrates **8–11** and products **12–15** of *PpYerE*-catalyzed transformations. Conditions: ketone **8–11** (20 mM), pyruvate (**6**, 50 mM), *PpYerE* (1 mg mL⁻¹), KP, buffer (50 mM, pH 8.0, containing 3 mM MgCl₂, 0.5 mM ThDP), 20% DMSO [only added for assays with β -tetralone (**10**) and 1-phenoxypropan-2-one (**11**)], total volume 1.5 mL,^[a] cyclohexane-1,2-dione (**9**, 100 mM), pyruvate (**6**, 20 mM). Conversions [%] were determined after 24 h by GC–MS analysis; ee values [%] (in brackets) were determined by chiral-phase HPLC analysis (n.d.: not determined). Results for *YpYerE* were published by Lehwald et al. and added for comparison.^[2]

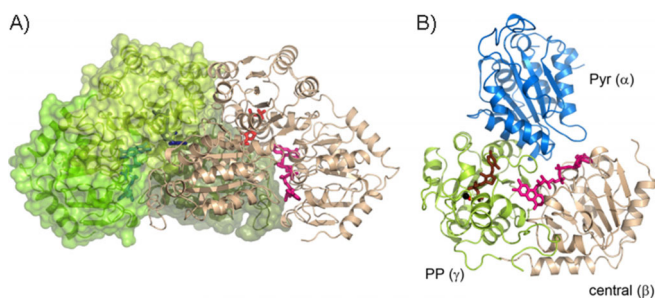


Figure 2. Overall structure of *PpYerE*. A) The *PpYerE* dimer. Both subunits are shown in cartoon representation, with subunit A colored cream, and subunit B colored in different shades of green for the three distinct domains (Pyr, forest green; central, mid-green; PP, lime green) and covered by a correspondingly colored semitransparent surface. The cofactors are shown as sticks, with ThDP in red and dark blue and FAD in pink and cyan for subunits A and B, respectively. B) The *PpYerE* subunit in cartoon representation. The three distinct domains are labeled and colored differently. ThDP and FAD are shown as sticks in brown and hot pink, respectively. The magnesium ion is shown as a black sphere, and the metal-coordinating water molecule is shown as a red sphere. Amino acids connecting the Pyr and central domains are not resolved in electron density.

viations are observed in the central FAD-binding domain and regions involved in subunit interface formation. The DALI

server identifies the homotetrameric *A. thaliana* AHAS, the search model used in molecular replacement, as the closest structural homologue, with a *Z*-score of 43.4 (PDB ID: RMSD = 2.2 Å for 539 aligned C _{α} positions).

ThDP binding

Binding of the ThDP cofactor is mediated by the Pyr and PP domains, with residues of the former surrounding the pyrimidine ring, whereas the diphosphate is, primarily via an Mg²⁺ ion, anchored in the PP domain of the other subunit, which results in binding of two ThDP molecules per homodimer. The two hydrogen bonds between the protein and the ThDP pyrimidine ring, formed by E48 to the N1' atom and by G420 to the N4' atom, are crucial for catalytic activity. They are conserved in almost all ThDP-dependent enzymes and are known to induce the 1',4'-imino tautomer^[15] and to orient the 4'-imino group, which facilitates deprotonation of the thiazolium C2 atom to a carbanion as the first step in the reaction cycle. In *PpYerE*, M422 is the hydrophobic residue that stabilizes the canonical V conformation of the ThDP.

For the present structure of *PpYerE*, additional electron density was observed to extend from the thiazolium ring of ThDP, and this is indicative of covalent attachment of an unknown moiety, possibly an oxygen atom (Figure 3). Thiazolone derivatives of ThDP have also been observed in other crystal structures of ThDP-dependent enzymes and are likely a result of exposure to intense X-ray radiation during data collection.^[17]

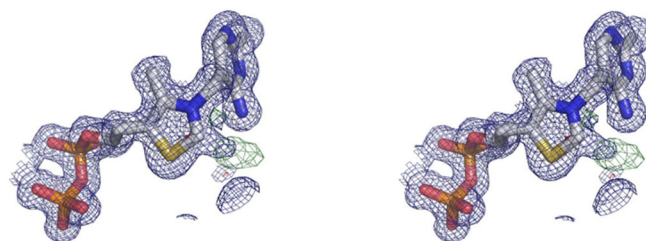


Figure 3. ThDP modification observed in the crystal structure of *PpYerE*. Stereoview of the final $2F_o - F_c$ map contoured at 1σ (blue) and the final $F_o - F_c$ map contoured at $+3\sigma$ (green) and -3σ (red) around ThDP. Both maps indicate modification of the cofactor at the C2 position.

FAD binding

FAD is located in a deep crevice at the interface between all three domains, with most of the enzyme residues involved in its binding originating from the central domain, which is, therefore, also termed the FAD-binding domain. The surface of this crevice is covered by an approximately 20-residue segment inserted between β 4 strand and α 5 helix of the Pyr domain that protrudes from the second subunit in the dimer. It largely sequesters what would otherwise be the more exposed face of the flavin cofactor from the surrounding solvent. FAD is bound in an extended conformation with the flavin ring placed near the thiazolium ring of ThDP; this is basically identical to the conformation observed in the crystal structures of other flavin-containing ThDP-dependent enzymes.^[18] All resi-

dues located within van der Waals distance to the FAD are shown in Figure S3.

As for ScAHAS, no catalytic function for FAD has been discerned, as no electron transfer to or from FAD is required for the catalyzed carbonylation reaction. The hypothesis of FAD being an evolutionary relict from POX-like ancestors formulated for AHAS by Chang and Cronan may thus also apply to FAD binding by *PpYerE*.^[19]

The substrate-binding site

The active site can be accessed by substrates through a relatively narrow tunnel, the walls of which are formed by residues from the PP- and FAD-binding domains of one subunit and the Pyr domain of the other subunit. The catalytically crucial C2 and N4' atoms of ThDP and the C7 methyl group of FAD are thereby the most solvent exposed. Part of helix α 22 and the following loop that contribute to formation of the active-site entrance are disordered in the B subunit, which does, however, not affect the regions of the active site nearest to the cofactors (Figure 4). It is feasible that partial disorder of this residue stretch is indicative of mobility with functional importance, for example, in terms of facilitating exchange of products by sub-

strates after the reaction has occurred and closing off the active site during catalysis or of adjusting active-site dimensions to the sizes and shapes of different acceptor substrates, especially as the corresponding residue stretch in the crystal structure of ScAHAS is also partially disordered.

In the immediate vicinity of the cofactors, the active site of *PpYerE* is highly similar to that of AtAHAS (Figure 4). From the residues forming this part of the cavity, all but L22' and I23' are conserved at (almost) the same positions in the two enzymes. The degree of sequence conservation is significantly lower at the outskirts of the substrate-binding cavity towards the herbicide-binding site identified for plant (and also yeast) AHAS. Here, the *PpYerE* residues M26, F482, and Y264 are replaced by alanine, tryptophan, and histidine, respectively, which may indicate differing substrate specificities or inhibition behavior of both enzymes.

Mutagenesis studies to invert enantioselectivity

PpYerE catalyzes the formation of (*R*)-PAC (**7a**) with high enantioselectivity (Table 1), and this can be explained by parallel orientation of the side chains of the donor (pyruvate, **6**) and acceptor (benzaldehyde, **5a**) prior to C–C bond formation.^[21] In

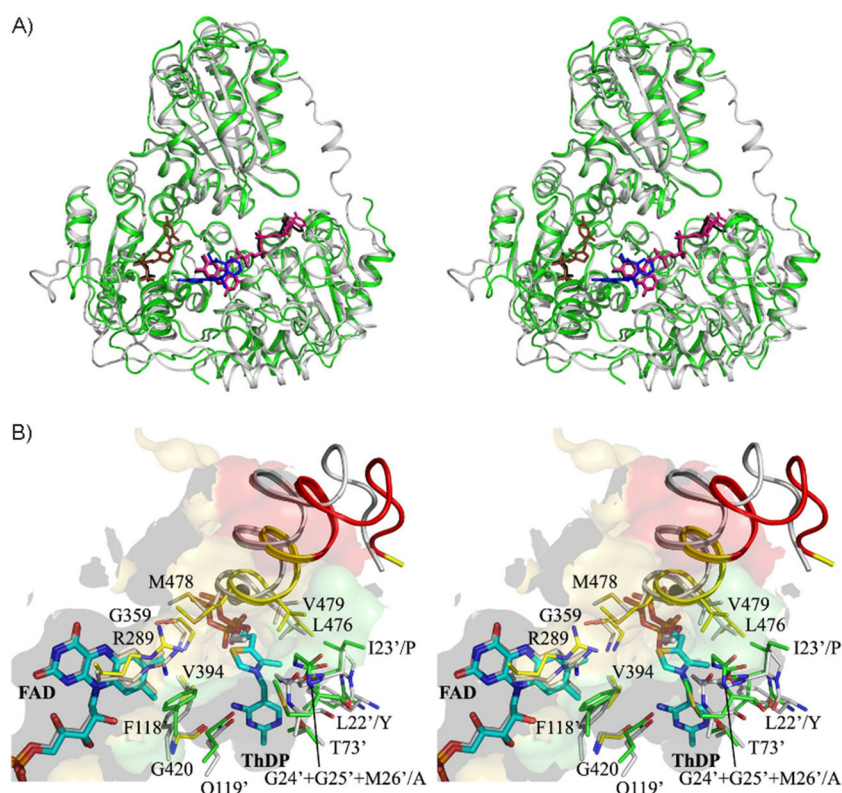


Figure 4. Comparison of *PpYerE* with AtAHAS (PDB ID: 1Y10).^[20] A) Stereoview of the superimposed subunits of *PpYerE* (green) and AtAHAS (gray) in cartoon representation. ThDP and FAD bound to *PpYerE* are shown as sticks in brown and pink, respectively. The sulfonyleurea-type inhibitor bound to the AtAHAS crystal structure selected for the superimposition is shown as sticks in blue, and the ThDP derivative and FAD are shown as black sticks. B) Stereoview of the superimposed *PpYerE* and AtAHAS substrate-binding sites. The substrate- and cofactor-binding cavity of *PpYerE* is outlined by a semitransparent surface, and all *PpYerE* residues forming its walls near the substrate-binding site are shown with carbon atoms in yellow if derived from subunit A and in green if belonging to subunit B. ThDP and FAD are depicted with carbon atoms in cyan. Helix 22 is shown as a cartoon, with the residue stretch not resolved in electron density in one of the subunits indicated in red. The corresponding AtAHAS secondary structure element is shown in white, and cofactors and amino-acid residues with carbon atoms are shown in white. The labels indicate the *PpYerE* residue, with the residue type of the corresponding AtAHAS residue given after a slash only if it is not conserved.

many ThDP-dependent decarboxylases, a potential antiparallel acceptor-binding pocket (also referred to as the "S-pocket") has been found that is blocked by amino-acid side chains.^[22] The pocket can be opened by a few amino-acid exchanges, enabling antiparallel orientation of substrate side chains, which is a prerequisite for *S* selectivity. This concept was successfully applied to the *R*-selective pyruvate decarboxylase from *Acetobacter pasteurianus* (*ApPDC*) as well as 2-succinyl-5-enolpyruvyl-6-hydroxy-3-cyclohexene-1-carboxylate synthase from both *Escherichia coli* and *B. subtilis* (*EcMenD*, *BsMenD*) to yield *S*-selective variants.^[23,24]

In *PpYerE*, the *S*-pocket is defined by L22, I23, G24, G25, L476, and V479 (see Figure S2A). V479 is located at the standard position 477 (according to the standard numbering scheme for ThDP-dependent decarboxylases of the BioCatNet database system), which was found to be decisive for the inversion of enantioselectivity of *ApPDC*, *EcMenD*, and *BsMenD*.^[25] In *PpYerE*, the size of the *S*-pocket is restricted by the backbone of helix α 22 that is shifted by about 2 Å into the area of the potential pocket compared to *ApPDC*. Modeling of benzaldehyde (**5a**) into a pocket that was opened by exchange of V479 to alanine and glycine, respectively, indicated that the available space was not sufficient for antiparallel binding of **5a**, as it clashed with the α -helix (Figure S2B). This was confirmed by experimental results in which the *ee* value of (*R*)-PAC (**7a**) was not altered for the variant V479G and was only slightly reduced for variant V479A (Table 2). Consequently, propanal (**16**) and *n*-pentanal (**17**) were tested as smaller, aliphatic acceptors. The respective products, 3-hydroxypentan-2-one (**19**) and 3-hydroxyheptan-2-one (**20**), are nature-identical flavor ingredients used for aroma production.^[26] The absolute configuration was determined by circular dichroism (CD) spectroscopy, in accordance with the spectrum of (*R*)-**19** recorded by Vinogradov et al. (Figure S3).^[27]

With respect to the product 3-hydroxypentan-2-one (**19**), wild-type *PpYerE* catalyzed the formation of the *S* enantiomer with 40% *ee*, which could be further increased to 57% *ee* by the mutation V479A. Mutation V479G, on the other hand, inverted the enantioselectivity to an excess of the *R* enantiomer (55% *ee*; Table 2). For product 3-hydroxyheptan-2-one (**20**), wild-type *PpYerE* gave a low excess (16%) of the *R* enantiomer. Again, mutation V479A increased the relative amount of the *S* enantiomer (31% *ee*), whereas mutation V479G increased the relative amount of the *R* enantiomer (29% *ee*; Table 2). Wild-type *PpYerE* showed a high *n*-pentanal (**17**) conversion of 98% within 1 h. The conversions with variants V479A and V479G were reduced to 30 and 14%, respectively, indicating lower enzymatic activity and/or stability of the variants.

From the acceptor ketones described above, hexane-3,4-dione (**18**) was selected for further investigations with the *PpYerE* variants, as it is less sterically demanding than benzaldehyde (**5a**) and, therefore, could theoretically fit into the engineered acceptor-binding pocket. Owing to the nomenclature based on the CIP priority rules, parallel orientation of the donor side chain and the longer acceptor side chain of **18** (–COCH₂CH₃) before C–C bond formation results in the formation of the *S* enantiomer. It was thus expected that opening of

the *S*-pocket would increase the formation of the *R* enantiomer of 3-hydroxy-3-ethylhexane-2,4-dione (**21**). Wild-type *PpYerE* showed low enantioselectivity, which was inverted for variant V479A; *ee* values for both conversions were below 30%. Variant V479G gave almost racemic **21**.

Even though high enantioselectivities could not be obtained, variant V479A showed a shift in the enantioselectivity towards increased formation of the *S* product in all reactions. This indicates that the pocket concept is generally applicable, although a high percentage of the acceptor substrate still binds in parallel orientation. The enantioselectivity of the variants could probably be increased by destabilization of the parallel orientation, as described by Westphal et al.^[24]

Interestingly, for variant V479G the enantioselectivity was shifted towards the *R* product if propanal (**16**) and *n*-pentanal (**17**) were used as acceptor substrates, even though more space should be available within the alternative acceptor-binding pocket. This might be due to an accumulation of glycine residues, as glycine is also found in positions 477 and 481 in helix α 22 as well as in positions 24 and 25, which line the potential pocket (Figure S2A). It can be assumed that introduction of another glycine destabilizes the secondary structure and leads to disintegration of the *S* pocket.

As exchange of V479 by alanine and glycine did not result in effective opening of the *S* pocket in *PpYerE*, other amino acids lining the pocket were exchanged to smaller residues, but this was also not successful, as tested for products 3-hydroxypentan-2-one (**19**) and 3-hydroxyheptan-2-one (**20**). Replacement of L476 by alanine and glycine yielded inactive variants. Exchange of I23 by alanine and glycine did not have a significant impact on the *ee* of **19** and increased the formation of the *R* enantiomer for **20**.

Conclusion

Although many ThDP-dependent enzymes catalyze carbonylation reactions of pyruvate as a donor with aldehydes as acceptors, only few ThDP-dependent enzymes, such as *YpYerE* and *PpYerE* (59% amino acid identity), utilize ketones to form tertiary alcohols. The numerous attempts to crystallize *YpYerE* have not been successful; nevertheless, we were able to crystallize *PpYerE* and determine its structure to 1.55 Å resolution. *PpYerE* displayed catalytic activity similar to that shown by *YpYerE*, that is, benzaldehyde and its derivatives in addition to cyclic and acyclic ketones and 1,2-diketones as acceptors and pyruvate as a donor were converted into the respective secondary and tertiary 2-hydroxy ketones. In the frame of site-directed mutagenesis studies, the *S*-pocket concept could also be applied to *PpYerE* but was limited for larger acceptor substrates owing to the structurally restricted size of the pocket.

Detailed structural and catalytic characterization of *PpYerE* and comparison with homologous *YpYerE* showed that both enzymes share the same amino-acid residues in their active sites, have very similar substrate ranges, and are encoded by genes that are located in highly similar biosynthetic gene clusters. Hence, our results pave the way for the identification of putatively related enzymes that should also be able to accept

ketones as substrates. Moreover, rational modification of ThDP-dependent decarboxylases and related enzymes resulting in ketone-accepting enzymes, as previously shown by Loschonsky et al.^[12] for the variant CDH-H28A/N484A, could enlarge the product range towards sterically demanding 2-hydroxy ketones.

Experimental Section

Construction of plasmids for gene expression: The gene *ilvB* (*ppYerE*, UniProtKB accession number Q4K6F7_PSEF5) was amplified by PCR according to standard protocols from the genomic DNA isolated from *Pseudomonas protegens* Pf-5 that was kindly provided by the Department of Environmental Systems Science ETH (Zurich, Switzerland). Therefore, the forward primer 5'-AATAA TCATA TGAAA GCCTC GGATG CAGTA GC-3' introducing an NdeI restriction site and the reverse primer 5'-AATAA TGCGG CCGCT CCATC GTGTC GGGGT GATTG-3' introducing a NotI restriction site were used (restriction sites underlined). The PCR product was then inserted into the expression vector pET22b(+) through restriction and ligation steps, which resulted in the plasmid pET22b*Pf-5 that contained the gene coding for the target protein IlvB (*PpYerE*) with a His₆ tag attached at the C terminus. Moreover, to obtain the N-terminally His₆-tag-carrying protein variant, the gene was further subcloned into the pET28a(+) expression vector. For this purpose, pET22b*Pf-5 was used as a template, and the gene was amplified by PCR by using the forward primer 5'-TATAT ATACA TATGA AAGCC TCGGA TGCAG TAGC-3' and the reverse primer 5'-TATAT AGGAT CCTTA TCCAT CGTGT CGGG-3' harboring NdeI and BamHI restriction sites (underlined), respectively. This amplified cDNA was inserted into the vector backbone in a manner similar to that described above to yield vector pET28b*Pf-5 encoding the target protein IlvB (*PpYerE*) with an N-terminal His₆ tag. In-frame cloning and correctness of the sequence of the genes in all vector constructs used for further experiments were confirmed by DNA sequencing (GATC Biotech, Germany). For plasmid amplification, *E. coli* DH5 α cells were used routinely.

Expression of the gene *ppYerE* constructs: After transformation of pET22b*Pf-5 or pET28b*Pf-5 into BL21(DE3) cells, single clones were used to inoculate 20 mL lysogeny broth (LB) nutrient medium containing 100 $\mu\text{g mL}^{-1}$ ampicillin or 50 $\mu\text{g mL}^{-1}$ kanamycin, respectively (representative example). These cultures were grown overnight at 37 °C under agitation (120–180 rpm). After dilution (1:100) in LB medium, 1 L cultures were cultivated under aerobic conditions in baffled flasks at 37 °C with agitation (120–180 rpm) until an optical density (OD₆₀₀) of 0.6 was reached. Then, isopropyl- β -D-thiogalactopyranoside (IPTG) was added to a final concentration of 0.1 mM and expression was performed overnight at 25 °C and 120–180 rpm. Cells were harvested by centrifugation at 6000 g at 4 °C for 45–60 min. Lysis of the cells was accomplished by sonication (duty cycle = 50%, control = 5, Sonifier 250, Branson, Danbury USA) by using 30 s pulses (3 \times), each with intervals of 30 s on ice in between (in KP₁ buffer A: 100 mM, pH 8.0 containing 0.5 mM ThDP, 3 mM MgCl₂). Alternatively, cells were lysed by using CellLytic B Cell Lysis Reagent (Sigma–Aldrich) and incubation for 30–60 min at 200 rpm and 37 °C. Cell debris was removed by centrifugation (6000 g at 4 °C for 45–60 min). The supernatant was used for purification of the target protein by immobilized metal-ion affinity chromatography (IMAC) on an Ni-NTA matrix by using KP₁ buffer B (50 mM, pH 8.0 containing 0.5 mM ThDP and 3 mM MgCl₂ supplemented with different concentrations of imidazole: 20 and 50 mM for the consecutive washing steps and 300 mM for elu-

tion of the target protein). The target protein eluate was desalted by using PD-10 columns (Sephadex G-25M, GE Healthcare) according to a protocol of the manufacturer and using KP₁ buffer A. For crystallization, target proteins were purified through an additional step by gel-permeation chromatography. Thus, a Superdex S200 10/300 column was equilibrated overnight with Tris buffer (20 mM, 3 mM MgCl₂, 1 mM ThDP, pH 8.0) and a flow rate of 0.3 mL min⁻¹. After loading the protein sample obtained from the previous IMAC purification and additional desalting, the flow rate was increased to 0.5 mL min⁻¹. The target protein appeared as dimers in solution, and the respective fractions were collected, pooled, and then concentrated by using Amicon Ultra centrifugal filter units (30 K) and Vivaspin 6 centrifugal devices (30 K), each at 3700 g for 25 min at 4 °C. Purification to homogeneity was confirmed by SDS-PAGE analysis. Full functionality of the enzymes was demonstrated by measuring activity towards a range of substrates for both the C-terminally and N-terminally His₆-tagged enzymes.

Site-directed mutagenesis: *PpYerE* variants were created with a PCR-based method by using synthetic mutagenic primers and the KOD Hot Start Polymerase Kit (Novagen). PCR reactions were performed in 50 μL and contained template DNA (3 ng μL^{-1}), primer (0.5 μM), dNTP mix (200 μM), MgSO₄ (1.5 mM), and KOD polymerase (0.02 U μL^{-1}). The PCR temperature profile was: initial denaturation at 95 °C for 120 s, followed by 18 cycles of denaturation (95 °C for 20 s), annealing (62 °C for 30 s), and elongation (72 °C for 220 s). A final elongation step at 72 °C for 10 min was added. After the PCR, reaction samples were purified by using the GeneJET PCR Purification Kit (Thermo Scientific) according to the manufacturer's information. Parental DNA was removed by DpnI digestion on a 20 μL scale. DNA (≤ 50 ng μL^{-1}) was incubated with FastDigest DpnI (1 μL , Thermo Scientific) at 37 °C for 3 h. Subsequently, a sample (8 μL) was used to transform chemically competent *E. coli* DH5 α cells (Thermo Scientific) according to a standard protocol. Individual colonies were cultivated in LB medium overnight, and plasmids were isolated with the QIAprep Spin Miniprep Kit (Qiagen). Gene sequences were confirmed by DNA sequencing (LGC Genomics, Berlin).

Biocatalytic transformations: For all carbonylation reactions, purified and lyophilized *PpYerE* variants were used. The final protein concentration was adjusted to 1 mg mL⁻¹. The preparations were incubated at 30 °C. Samples were analyzed by chiral-phase HPLC after dilution in acetonitrile or chiral-phase GC–MS after extraction with ethyl acetate (Supporting Information). Buffer conditions and substrate concentrations depended on the respective acceptor substrate:

Transformations comparing *YpYerE* and *PpYerE* (Table 1 and Scheme 1)

Pyruvate (6) + *benzaldehydes* 5a–f: 50 mM Potassium phosphate, 0.5 mM ThDP, 3 mM MgCl₂, 50 mM pyruvate (6), 20 mM benzaldehyde or derivative 5a–f, *YpYerE* (crude extract), 20–30% DMSO, pH 8.0.

Pyruvate (6) + *ketones* 8–11: 50 mM Potassium phosphate, 0.5 mM ThDP, 3 mM MgCl₂, 50 mM pyruvate (6), 20 mM ketone 8–11, 20% DMSO (only added for assays with β -tetralone (10) and 1-phenoxypropan-2-one (11), pH 8.0.

Transformations with variants (Table 2)

Pyruvate (6) + *benzaldehyde* (5a): 50 mM Potassium phosphate, 0.5 mM ThDP, 3 mM MgCl₂, 50 mM pyruvate (6), 20 mM benzaldehyde (5a), pH 8.

Pyruvate (**6**) + aliphatic aldehydes **16** and **17**: 100 mM Potassium phosphate, 2.4 mM ThDP, 3 mM MgCl₂, 50 μM FAD, 50 mM pyruvate (**6**), 50 mM propanal (**16**), and *n*-pentanal (**17**), pH 8.

Pyruvate (**6**) + hexane-3,4-dione (**18**): 100 mM Potassium phosphate, 2.4 mM ThDP, 3 mM MgCl₂·6H₂O, 50 μM FAD, 50 mM pyruvate (**6**), 20 mM hexane-3,4-dione (**18**), pH 7.

Crystallization: Initial crystallization screens were performed by using 96-well sparse matrix screens in sitting-drop setups at 20 °C. Several hits obtained with the Morpheus crystallization screen (Molecular Dimensions) were further optimized. The crystal used for data collection was obtained by sitting-drop vapor diffusion against a 1 mL reservoir containing 10% (w/v) PEG-4000, 0.1 M 2-(*N*-morpholino)ethanesulfonic acid (MES)/imidazole pH 6.5, 0.3 M MgCl₂, 0.3 M CaCl₂, and 17% (v/v) glycerol at 20 °C. The 1 μL drop consisted of equal volumes of reservoir and protein solution (10.3 mg mL⁻¹ PpYerE in Tris (20 mM, pH 8.0), 3 mM MgCl₂, 1 mM ThDP). Crystals appeared within 1 day of equilibration.

Data collection, structure determination, and refinement: Crystals were flash frozen without additional cryoprotection by rapid transfer into liquid nitrogen. Crystallographic data were collected at 100 K at beamline 14.1 of the Berliner Elektronenspeicherring-Gesellschaft für Synchrotronstrahlung (BESSY) (Berlin, Germany). Details of data collection and refinement statistics are given in Table S1. The data were originally indexed in space group C222₁, but subsequent analysis revealed them to be twinned (twin operator $-l, -k, -h$; twin fraction = 0.44). The crystal thus belongs to space group P2₁ with unit-cell parameters of $a = c = 65.3$ Å, $b = 139.9$ Å, $\beta = 97.9^\circ$ and contains two polypeptide chains (one homodimer) per asymmetric unit. Integration of the diffraction data was performed with iMOSFLM.^[28] Intensities were merged and scaled by using AIMLESS,^[29] and structure factor amplitudes were calculated with CTRUNCATE of the CCP4 suite of programs.^[30]

Phases were obtained by molecular replacement by using PHASER^[31] with a high-resolution limit of 2.5 Å and a subunit of *Arabidopsis thaliana* acetoxy acid synthase (PDB ID: 1YBH, 32% sequence identity)^[20] as search model.

After initial rigid body and restraint refinement and extension of the phases to 1.55 Å resolution, iterations of model building in COOT^[32] were alternated with TLS and restrained refinement with intensity-based twin refinement in REFMAC5^[33] until the crystallographic *R* factor and *R*_{free} converged. All reflections in the given resolution range (Table S1) were used with the exception of 5% randomly selected reflections for monitoring *R*_{free}. Automatically determined local NCS restraints were applied. Water molecules were added manually or by using the search routine implemented in COOT.

The refined model contains residues 1–182 and 193–565 and residues 1–181, 195–482, and 492–568 for chains A and B, respectively; two ThDP; two FAD; two Mg²⁺; and 876 water molecules. It has excellent stereochemistry, as determined with RAMPAGE^[34] and MOLPROBITY,^[35] with 98.8% of the residues in the favored region and none in outlier regions of the Ramachandran plot, respectively. Further details about model quality are given in Table S1. Structure comparisons and similarity searches were performed by using the DALI server^[36] and PDBeFOLD^[37] at the European Bioinformatics Institute (<http://www.ebi.ac.uk/msd-srv/ssm>). Molecular surfaces were analyzed with the Protein Interfaces, Surfaces, and Assemblies Service at the European Bioinformatics Institute.^[38] Figures 2–4 were prepared with PyMOL (<http://www.pymol.org>). The crystallo-

graphic data and structure were deposited in the Protein Data Bank under ID: 5AHK.

Acknowledgements

We thank Sascha Ferlaino, Dr. Maryam Beigi, and Dr. Tobias Wacker, University of Freiburg, for technical support and helpful discussions; Ömer Poyraz, Karolinska Institutet, for collection of the crystallographic data; and Dr. Kay Greenfield for help in improving the manuscript. We acknowledge access to synchrotron radiation at BESSY, Berlin, Germany, and thank the staff at beamline ID14-1 for support. This work was supported by a grant from the Swedish Research Council (to G.S.), by grants from the Deutsche Forschungsgemeinschaft (DFG; FOR 1296), and by a grant from the European Union's Horizon 2020 Research and Innovation Programme under Grant Agreement no. 635595.

Conflict of Interest

The authors declare no conflict of interest.

Keywords: asymmetric synthesis • biocatalysis • biosynthesis • C–C coupling • tertiary alcohols

- [1] H. Chen, Z. Guo, H.-w. Liu, *J. Am. Chem. Soc.* **1998**, *120*, 11796.
- [2] P. Lehwald, M. Richter, C. Röhr, H.-w. Liu, M. Müller, *Angew. Chem. Int. Ed.* **2010**, *49*, 2389; *Angew. Chem.* **2010**, *122*, 2439.
- [3] H. Grisebach, R. Schmid, *Angew. Chem. Int. Ed. Engl.* **1972**, *11*, 159; *Angew. Chem.* **1972**, *84*, 192.
- [4] P. P. Giovannini, P. Pedrini, V. Venturi, G. Fantin, A. Medici, *J. Mol. Catal. B* **2010**, *64*, 113.
- [5] G. Bernacchia, O. Bortolini, M. de Bastiani, L. A. Lerin, S. Loschonsky, A. Massi, M. Müller, P. P. Giovannini, *Angew. Chem. Int. Ed.* **2015**, *54*, 7171; *Angew. Chem.* **2015**, *127*, 7277.
- [6] P. P. Giovannini, G. Fantin, A. Massi, V. Venturi, P. Pedrini, *Org. Biomol. Chem.* **2011**, *9*, 8038.
- [7] a) O. Bortolini, P. P. Giovannini, S. Maietti, A. Massi, P. Pedrini, G. Sacchetti, V. Venturi, *J. Mol. Catal. B* **2013**, *85–86*, 93; b) P. P. Giovannini, O. Bortolini, A. Cavazzini, R. Greco, G. Fantin, A. Massi, *Green Chem.* **2014**, *16*, 3904.
- [8] P. P. Giovannini, L. A. Lerin, M. Müller, G. Bernacchia, M. de Bastiani, M. Catani, G. Di Carmine, A. Massi, *Adv. Synth. Catal.* **2016**, *358*, 2767.
- [9] T. Sehl, S. Bock, L. Marx, Z. Maugeri, L. Walter, R. Westphal, C. Vogel, U. Menyes, M. Erhardt, M. Müller, M. Pohl, D. Röther, *Green Chem.* **2017**, *19*, 380.
- [10] X. Jiang, H. Zhang, J. Yang, Y. Zheng, D. Feng, W. Liu, X. Xu, Y. Cao, H. Zou, R. Zhang, T. Cheng, F. Jiao, M. Xian, *Sci. Rep.* **2013**, *3*, 2445.
- [11] S. Loschonsky, S. Waltzer, S. Fraas, T. Wacker, S. L. A. Andrade, P. M. H. Kroneck, M. Müller, *ChemBioChem* **2014**, *15*, 389.
- [12] S. Loschonsky, T. Wacker, S. Waltzer, P. P. Giovannini, M. J. McLeish, S. L. A. Andrade, M. Müller, *Angew. Chem. Int. Ed.* **2014**, *53*, 14402; *Angew. Chem.* **2014**, *126*, 14630.
- [13] *Geneious alignment* (alignment with free ends and gaps, cost matrix: blosum62, gap open penalty: 12, gap extension penalty: 3, Geneious).
- [14] J. S. Thorson, S. F. Lo, H. W. Liu, *J. Am. Chem. Soc.* **1993**, *115*, 5827.
- [15] V. P. Miller, J. S. Thorson, O. Ploux, S. F. Lo, H. W. Liu, *Biochemistry* **1993**, *32*, 11934.
- [16] a) M. Müller, G. A. Sprenger, M. Pohl, *Curr. Opin. Chem. Biol.* **2013**, *17*, 261; b) M. Beigi, E. Gauchenova, L. Walter, S. Waltzer, F. Bonina, T. Stillger, D. Rother, M. Pohl, M. Müller, *Chem. Eur. J.* **2016**, *22*, 13999.
- [17] C. L. Berthold, P. Moussatche, N. G. J. Richards, Y. Lindqvist, *J. Biol. Chem.* **2005**, *280*, 41645.
- [18] S. S. Pang, R. G. Duggleby, L. W. Guddat, *J. Mol. Biol.* **2002**, *317*, 249.

- [19] Y. Y. Chang, J. E. Cronan, *J. Bacteriol.* **1988**, *170*, 3937.
- [20] J. A. McCourt, S. S. Pang, J. King-Scott, L. W. Guddat, R. G. Duggleby, *Proc. Natl. Acad. Sci. USA* **2006**, *103*, 569.
- [21] M. Knoll, M. Müller, J. Pleiss, M. Pohl, *ChemBioChem* **2006**, *7*, 1928.
- [22] P. T. Anastas, *Handbook of Green Chemistry*, Wiley-VCH, Weinheim, **2010**.
- [23] a) R. Westphal, S. Waltzer, U. Mackfeld, M. Widmann, J. Pleiss, M. Beigi, M. Müller, D. Rother, M. Pohl, *Chem. Commun.* **2013**, *49*, 2061; b) R. Westphal, S. Jansen, C. Vogel, J. Pleiss, M. Müller, D. Rother, M. Pohl, *ChemCatChem* **2014**, *6*, 1082; c) D. Rother (née Gocke), G. Kolter, T. Gerhards, C. L. Berthold, E. Gauchenova, M. Knoll, J. Pleiss, M. Müller, G. Schneider, M. Pohl, *ChemCatChem* **2011**, *3*, 1587.
- [24] R. Westphal, D. Hahn, U. Mackfeld, S. Waltzer, M. Beigi, M. Widmann, C. Vogel, J. Pleiss, M. Müller, D. Rother, M. Pohl, *ChemCatChem* **2013**, *5*, 3587.
- [25] a) C. Vogel, M. Widmann, M. Pohl, J. Pleiss, *BMC Biochem.* **2012**, *13*, 24; b) P. C. F. Buchholz, C. Vogel, W. Reusch, M. Pohl, D. Rother, A. C. Spieß, J. Pleiss, *ChemBioChem* **2016**, *17*, 2093.
- [26] a) *Flavour Science: Recent Developments* (Eds.: A. J. Taylor, D. S. Mottram), The Royal Society of Chemistry, Cambridge, **1996**; b) F. Neuser, H. Zorn, R. G. Berger, *J. Agric. Food Chem.* **2000**, *48*, 6191.
- [27] M. Vinogradov, A. Kaplun, M. Vyazmensky, S. Engel, R. Golbik, K. Tittmann, K. Uhlemann, L. Meshalkina, Z. Barak, G. Hübner, D. M. Chipman, *Anal. Biochem.* **2005**, *342*, 126.
- [28] A. G. W. Leslie, H. R. Powell in *Evolving Methods for Macromolecular Crystallography* (Eds.: R. J. Read, J. L. Sussman), Springer, Dordrecht, **2007**, pp. 40–52.
- [29] P. R. Evans, *Acta Crystallogr. Sect. D Biol. Crystallogr.* **2011**, *67*, 282.
- [30] M. D. Winn, C. C. Ballard, K. D. Cowtan, E. J. Dodson, P. Emsley, P. R. Evans, R. M. Keegan, E. B. Krissinel, A. G. W. Leslie, A. McCoy, S. McNicholas, G. Murshudov, N. Pannu, E. Potterton, H. Powell, R. Read, A. Vagin, K. Wilson, *Acta Crystallogr. Sect. D Biol. Crystallogr.* **2011**, *67*, 235.
- [31] A. J. McCoy, R. W. Grosse-Kunstleve, P. D. Adams, M. D. Winn, L. C. Storoni, R. J. Read, *J. Appl. Crystallogr.* **2007**, *40*, 658.
- [32] P. Emsley, B. Lohkamp, W. G. Scott, K. Cowtan, *Acta Crystallogr. Sect. D Biol. Crystallogr.* **2010**, *66*, 486.
- [33] G. N. Murshudov, A. A. Vagin, E. J. Dodson, *Acta Crystallogr. Sect. D Biol. Crystallogr.* **1997**, *53*, 240.
- [34] S. C. Lovell, I. W. Davis, W. B. Arendall, P. I. W. de Bakker, J. M. Word, M. G. Prisant, J. S. Richardson, D. C. Richardson, *Proteins Struct. Funct. Bioinf.* **2003**, *50*, 437.
- [35] V. B. Chen, W. B. Arendall, J. J. Headd, D. A. Keedy, R. M. Immormino, G. J. Kapral, L. W. Murray, J. S. Richardson, D. C. Richardson, *Acta Crystallogr. Sect. D Biol. Crystallogr.* **2010**, *66*, 12.
- [36] L. Holm, L. M. Laakso, *Nucleic Acids Res.* **2016**, *44*, W351–W355.
- [37] E. Krissinel, K. Henrick, *Acta Crystallogr. Sect. D Biol. Crystallogr.* **2004**, *60*, 2256.
- [38] E. Krissinel, K. Henrick, *J. Mol. Biol.* **2007**, *372*, 774.

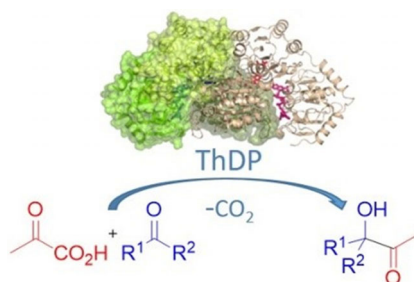
Manuscript received: June 18, 2018

Accepted manuscript online: August 13, 2018

Version of record online: ■ ■ ■ 0000

FULL PAPERS

tert alert! A thiamine diphosphate (ThDP)-dependent enzyme catalyzing the cross-condensation of a keto acid with several activated and nonactivated ketones gives chiral tertiary alcohols, products that are otherwise difficult to obtain in an enantioenriched form. To enable comparison of aldehyde-/ketone-accepting enzymes and to guide site-directed mutagenesis studies, we solved the crystal structure of this enzyme.



S. Hampel, J.-P. Steitz, A. Baierl,
P. Lehwald, L. Wiesli, M. Richter, A. Fries,
M. Pohl, G. Schneider, D. Dobritzsch,*
M. Müller*

■■ - ■■

Structural and Mutagenesis Studies of the Thiamine-Dependent, Ketone-Accepting YerE from *Pseudomonas protegens* 